

Long-range Lattice-Gas Algorithm

J. Yepez

Phillips Laboratory, Hanscom Field, Massachusetts 01731

(10 Oct 1994)

Abstract

Presented is a novel algorithmic method for simulating complex fluids, for instance multiphase single component fluids and molecular systems. The algorithm falls under a class of single-instruction multiple-data computation known as lattice-gases, and therefore inherits exact computability on a discrete spacetime lattice. Our contribution is the use of nonlocal interactions that allow us to model a richer set of physical dynamics, such as crystallization processes, yet to do so in a way that remains locally computed. A simple computational scheme is employed that allows all the dynamics to be computed in parallel with two additional bits of local site data, for outgoing and incoming messengers, regardless of the number of long-range neighbors. The computational scheme is an efficient decomposition of a lattice-gas with many neighbors. It is conceptually similar to the idea of virtual intermediate particle momentum exchanges that is well known in particle physics. All 2-body interactions along a particular direction define a spatial partition that is updated in parallel. Random permutation through the partitions is sufficient to recover the necessary isotropy as long as enough momentum exchange directions are used. The algorithm is implemented on the CAM-8 prototype.

Report Documentation Page

Form Approved
OMB No. 0704-0188

Public reporting burden for the collection of information is estimated to average 1 hour per response, including the time for reviewing instructions, searching existing data sources, gathering and maintaining the data needed, and completing and reviewing the collection of information. Send comments regarding this burden estimate or any other aspect of this collection of information, including suggestions for reducing this burden, to Washington Headquarters Services, Directorate for Information Operations and Reports, 1215 Jefferson Davis Highway, Suite 1204, Arlington VA 22202-4302. Respondents should be aware that notwithstanding any other provision of law, no person shall be subject to a penalty for failing to comply with a collection of information if it does not display a currently valid OMB control number.

1. REPORT DATE 10 OCT 1994		2. REPORT TYPE		3. DATES COVERED -	
4. TITLE AND SUBTITLE Long-Range Lattice-Gas Algorithm				5a. CONTRACT NUMBER	
				5b. GRANT NUMBER	
				5c. PROGRAM ELEMENT NUMBER	
6. AUTHOR(S)				5d. PROJECT NUMBER	
				5e. TASK NUMBER	
				5f. WORK UNIT NUMBER	
7. PERFORMING ORGANIZATION NAME(S) AND ADDRESS(ES) Phillips Laboratory,Hanscom Field,MA,01731				8. PERFORMING ORGANIZATION REPORT NUMBER	
9. SPONSORING/MONITORING AGENCY NAME(S) AND ADDRESS(ES)				10. SPONSOR/MONITOR'S ACRONYM(S)	
				11. SPONSOR/MONITOR'S REPORT NUMBER(S)	
12. DISTRIBUTION/AVAILABILITY STATEMENT Approved for public release; distribution unlimited					
13. SUPPLEMENTARY NOTES					
14. ABSTRACT Presented is a novel algorithmic method for simulating complex fluids, for instance multiphase single component fluids and molecular systems. The algorithm falls under a class of single-instruction multiple-data computation known as lattice-gases, and therefore inherits exact computability on a discrete spacetime lattice. Our contribution is the use of nonlocal interactions that allow us to model a richer set of physical dynamics, such as crystallization processes, yet to do so in a way that remains locally computed. A simple computational scheme is employed that allows all the dynamics to be computed in parallel with two additional bits of local site data, for outgoing and incoming messengers, regardless of the number of long-range neighbors. The computational scheme is an efficient decomposition of a lattice-gas with many neighbors. It is conceptually similar to the idea of virtual intermediate particle momentum exchanges that is well known in particle physics. All 2-body interactions along a particular direction define a spatial partition that is updated in parallel. Random permutation through the partitions is sufficient to recover the necessary isotropy as long as enough momentum exchange directions are used. The algorithm is implemented on the CAM-8 prototype.					
15. SUBJECT TERMS					
16. SECURITY CLASSIFICATION OF:			17. LIMITATION OF ABSTRACT	18. NUMBER OF PAGES 38	19a. NAME OF RESPONSIBLE PERSON
a. REPORT unclassified	b. ABSTRACT unclassified	c. THIS PAGE unclassified			

Contents

1	Introduction	1
2	The Cellular Automata Machine CAM-8	3
3	Lattice-Gas Automaton: An Exactly Computable Dynamical System	6
4	Isotropic Lattice Tensors	9
5	Triangular Lattice	10
6	Local Collision Rules	12
7	Long-Range 2-Body Interactions	14
8	A Simple Example: Bounce-Back Orbit	16
9	Another Example: Clockwise Orbit	20
10	Symmetries in Long Range Interactions	26
11	Central-Body Interaction Neighborhood and 2D Crystallization	27
12	Conclusion	29

List of Figures

1	MIT Laboratory for Computer Science CAM-8 Prototype	3
2	CAM-8 System Diagram	5
3	Hexagonal Lattice Convention	11
4	FHP Collision Rules	14
5	Bounce-Back and Clockwise Bound States	14
6	Liquid-Gas Phase Separation	24
7	Long-Range 2-Body Interactio Terms	25
8	Twelve Neighbors on a Triangular Lattice	27
9	Time Evolution of Crystallization in a Lattice-Gas with Multiple Fixed-Range Interactions	30

List of Tables

1	Simple right-handed collision table	13
2	Simple left-handed collision table	13
3	Lattice vector components	15
4	Long-range interaction sequence	20
5	Long-range interaction: double photon emission	23
6	Long-range interaction: double photon absorption	23

1 Introduction

To illustrate the how one may implement a lattice-gas with long-range interactions, let us consider for simplicity a two-dimensional example with a system having only one interaction range and consider only the case of an attractive interaction. The more general case of multiple interaction ranges with both repulsive and attractive interactions and in higher dimensions will follow directly. Specifically, we discuss our new molecular dynamics lattice-gas algorithm that uses eight interaction ranges and both repulsive and attractive interactions to approximate a Lenord-Jones intermolecular potential.

Our long-range lattice-gas has been implemented on the MIT cellular automata machine prototype, the CAM-8. Consequently, we first give a brief description of the CAM-8 architecture. We next give a brief description of what a lattice-gas automaton is and explain why it is an exactly computable representation of a dynamical system. One of the principle requirements for a lattice-gas with microscopic finite-point group symmetry to give rise to macroscopic continuous rotational symmetry is that the underlying lattice must be *isotropic*. Therefore we describe what it means for a lattice to be isotropic. Working in two-dimensions is much easier than working in three, both for implementing computer models and for describing them. For this reason we present our long-range lattice-gas algorithm in two-dimensions on the triangular lattice.

When introduced to the triangular lattice-gas model for the first time, one inevitably asks the following question: Why does the discrete dynamics fail to reproduce the correct continuum hydrodynamic limit when implemented on a

square lattice? One finds that four momentum states are insufficient by noting that the derivation of the Navier-Stokes equation relies on the expansion of the momentum flux density tensor in terms of the isotropic tensor E^4 which itself could be expanded in products of two-dimensional Kronecker deltas, given below in (10). For the square lattice case, the lattice vectors are orthogonal and E^4 cannot be decomposed into two-dimensional Kronecker deltas. Instead

$$E_{ijkl}^4|_{B=4} = 2\delta_{ijkl}$$

where δ_{ijkl} is a four-dimensional Kronecker delta illustrating the lack of isotropy of the momentum flux density on a square lattice-gas. Since five nearest neighbors is not space filling, the next possible choice is six or the triangular lattice. The simplest discrete dynamics in two-dimensions is known as a hexagonal lattice-gas or an FHP lattice-gas, after its originators Uriel Frisch, Brosl Hasslacher, and Yves Pomeau [1]. Since the long-range lattice-gas still retains local collisions, we present the simple FHP-model here for completeness. Next we introduce the long-range 2-body interaction, restricting ourselves to central-body attractive interactions, for the sake of simplicity. We discuss two different bound states, the bounce-back orbit and the clockwise orbit.

When implementing lattice-gas algorithms it is often useful try to find economical ways of expressing the collisions or interactions so as to reduce the size of a look-up table or reduce the depth of the logical representation of the algorithm. To this end we briefly discuss some symmetries inherent in long-range interactions, in particular we introduce parity and conjugation symmetries. Finally, we discuss our implementation of a multi-long-range lattice-gas. Remarkably,

this methodology allows us to model solid-state dynamics and as such offers an alternative to the usual method of computational molecular dynamics.

2 The Cellular Automata Machine CAM-8



Figure 1: MIT Laboratory for Computer Science cellular automata machine CAM-8. This 8 module prototype can evolve a D-dimensional cellular space with 32 million sites where each site has 16 bits of data with a site update rate of 200 million per second.

The cellular automata machine CAM-8 architecture devised by Norman Margolus of the MIT Laboratory for Computer Science [2, 3] is the latest in a line of cellular automata machines developed by the Information Mechanics Group at MIT [4, 5, 6]. It is optimized for performing lattice-gas simulations. The CAM-8 architecture itself is a simple abstraction of lattice gas dynamics. Lattice gas data streaming and collisions are directly implemented in the architecture. The

communication network is a cartesian three-dimensional mesh. Crystallographic lattice geometries can be directly embedded into the CAM-8. Each site of the lattice has a certain number of bits (a multiple of 16) which we refer to as a “cell”. Each bit of the cell, or equivalently each bit plane of the lattice, can be translated through the lattice in any arbitrary direction. The translation vectors for the bit planes are termed “kicks”. The specification of the x,y, and z components of the kicks for each bit plane (or hyperplane) exactly defines the lattice. The kicks can be changed during the simulation. Thus, the data movement in the CAM-8 is general. Once the kicks are specified, the coding of the lattice-gas streaming is completed. In effect, the kicks determine all the global permutations of the data.

Local permutations of data occur within the cells. These permutations are the computational metaphor for physical collisions between particles.¹ All local permutations are implemented in look-up tables. That is, all possible physical events with a certain input configuration and a certain output configuration are precomputed and stored in SRAM, for fast table look-up. The width of the CAM-8 look-up tables are limited to 16-bits, or 64K entries. This is a reasonable width satisfying the opposing considerations of model complexity versus memory size limitations for the SRAM. Site permutations of data wider than 16-bits must be implemented in several successive table look-up passes. Since the look-up tables are double buffered, a scan of the space can be performed while a new look-up table is loaded for the next scan.

¹Locally, the CAM-8 is not limited to performing only permutations, it can do general mappings. However, since we are interested in only particle conserving reversible dynamics,

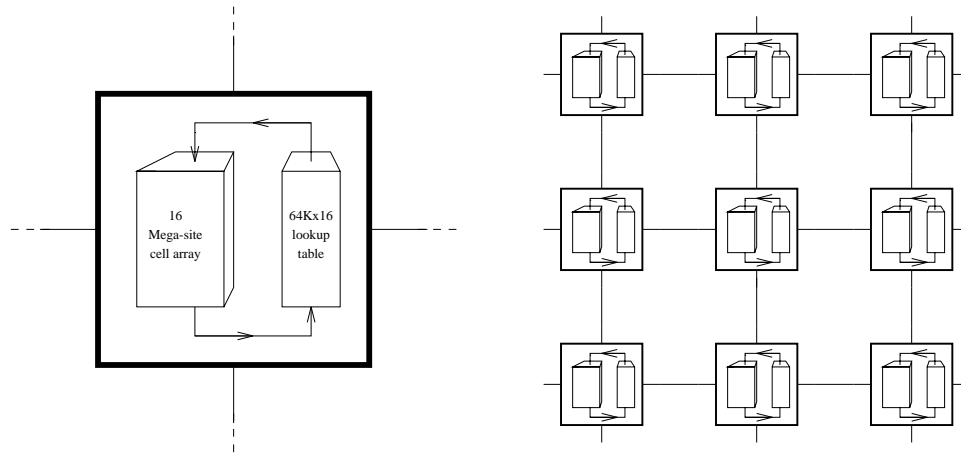


Figure 2: CAM-8 system diagram. (a) A single processing node, with DRAM site data flowing through an SRAM lookup table and back into DRAM. (b) Spatial array of CAM-8 nodes, with nearest-neighbor (mesh) interconnect (1 wire/bit-slice in each direction).

Figure 2 is a schematic diagram of a CAM-8 system. On the left is a single hardware module—the elementary “chunk” of the architecture. On the right is an indefinitely extendable array of modules (drawn for convenience as two-dimensional, the array is normally three-dimensional). A uniform spatial calculation is divided up evenly among these modules, with each module simulating a volume of up to millions of fine-grained spatial sites in a sequential fashion. In the diagram, the solid lines between modules indicate a local *mesh* interconnection. These wires are used for spatial data movements. There is also a tree network (not shown) connecting all modules to the front-end host, a SPARC workstation with a custom SBus interface card, controls the CAM-8. It downloads a bit-mapped pattern as the initial condition for the simulations. It also sends a “step-list” to the CAM-8 to specify the sequence of kicks and permutations are sufficient.

scans that evolve the lattice-gas in time. One can view the lattice-gas simulation in real-time since a custom video module captures site data for display on a VGA monitor, a useful feature for lattice-gas algorithm development, test and evaluation. The CAM-8 has built-in 25-bit event counters allowing real-time measurements without slowing the lattice-gas evolution. This feature is used to do real-time coarse-grain block averaging of the lattice-gas number variables and to compute the components of the momentum vectors for each block. The amount of coarse-grained data is sufficiently small to be transferred back to the front-end host for graphical display as an evolving flow field within an X-window.

3 Lattice-Gas Automaton: An Exactly Computable Dynamical System

A boolean formulation of an exactly computable dynamical system, known as a lattice-gas, may be stated in a way that is consistent with the Boltzmann equation for kinetic transport. In essence the lattice-gas dynamics are a simplified form of molecular transport as we restrict ourselves to a cellular phase space. The macroscopic equations, in particular the continuity equation and the Navier-Stokes equation, are obtained by coarse-graining over a discrete microdynamical transport equation for number boolean variables. The scheme employs the finite-point group symmetry of a crystallographic spatial lattice. It is somewhat inevitable that to obtain an exactly computable representation of fluid dynamics one must perform a statistical treatment over discrete number

variables.

Before introducing the basic lattice-gas microdynamical transport equation, let us give some notational conventions. We consider a spatial lattice with N total sites. The fundamental unit of length is the size of a lattice cell, l , and the fundamental unit of time, τ , is the time it takes for a speed-one particle to go from one lattice site to a nearest neighboring site. Particles, with unit mass m , propagate on the lattice. The unit lattice propagation speed is denoted by $c = \frac{l}{\tau}$. Particles occupy this discrete space and can have only a finite B number of possible momenta. The lattice vectors are denoted by e_{ai} where $a = 1, 2, \dots, B$. For example, for a single-speed gas on a triangular lattice, $a = 1, 2, \dots, 6$. A particle's state is completely specified at some time, t , by specifying its position on the lattice, x_i , and its momentum, $p_i = mce_{ai}$, at that position. The particles obey Pauli exclusion since only one particle can occupy a single momentum state at a time. The total number of configurations per site is 2^B . The total number of possible single particle momentum states available in the system is $N_{\text{total}} = BN$. With P particles in the system, we denote the filling fraction by $d = \frac{P}{N_{\text{total}}}$.

The number variable, denoted by $n_a(\mathbf{x}, t)$, takes the value of one if a particle exists at site \mathbf{x} at time t in momentum state $mc\hat{\mathbf{e}}_a$, and takes the value of zero otherwise. The evolution of the lattice-gas can then be written in terms of n_a as a two-part process: a collision and streaming part. The collision part reorders the particles locally at each site.

$$n'_a(\mathbf{x}, t) = n_a(\mathbf{x}, t) + \Omega_a(\vec{n}(\mathbf{x}, t)), \quad (1)$$

where Ω_a represents the collision operator and in general depends on all the particles, \vec{n} at the site. So as a short-hand we suppress the index on the occupation variable when it is an argument of $\Omega_a(\vec{n}(\mathbf{x}, t))$ to represent this general dependence. In the streaming part of the evolution the particle at position \mathbf{x} “hops” to its neighboring site at $\mathbf{x} + l\hat{\mathbf{e}}_a$ and then time is incremented by τ

$$n'_a(\mathbf{x} + l\hat{\mathbf{e}}_a, t + \tau) = n_a(\mathbf{x}, t) + \Omega_a(\vec{n}(\mathbf{x}, t)). \quad (2)$$

Equation (2) is the lattice-gas microdynamical transport equation of motion.

The collision operator can only permute the particles locally on the site since we wish the local particle number to be conserved before and after the collision.

That is,

$$n(\mathbf{x}, t) = \sum_a n'_a(\mathbf{x}, t) = \sum_a n_a(\mathbf{x}, t). \quad (3)$$

Equation (3) defines the local number density. Summing (2) over lattice directions then implies the following constraint on the collision operator

$$\sum_a \Omega_a = 0. \quad (4)$$

We may define the local momentum as

$$p_i(\mathbf{x}, t) = mc \sum_a e_{ai} n'_a(\mathbf{x}, t) = mc \sum_a e_{ai} n_a(\mathbf{x}, t), \quad (5)$$

which of course must also be conserved before and after a collision. Again, this imposes a constraint on the collision operator.

$$\sum_a e_a \Omega_a = 0. \quad (6)$$

As a matter of notation it should be understood that whenever a directionally dependent quantity is written, its subscripted index is taken modulo B. Using

the number variable, for example, it is understood that

$$n_{a+b} = n_{\text{mod } B(a+b)}. \quad (7)$$

As a short hand, a negative indice will represent the antiparallel direction, so since $\hat{\mathbf{e}}_{a+\frac{B}{2}} = -\hat{\mathbf{e}}_a$ we may write

$$n_{-a} = n_{a+\frac{B}{2}}. \quad (8)$$

4 Isotropic Lattice Tensors

We construct an n -th rank tensor composed of a product of lattice vectors [7]

$$E^{(n)} = E_{i_1 \dots i_n} = \sum_a (e_a)_{i_1} \cdots (e_a)_{i_n}, \quad (9)$$

where $a = 1, \dots, B$. All odd rank E vanish. We wish to express $E^{(2n)}$ in terms of Kronecker deltas, $\delta_{ij} = 1$ for $i = j$ and zero otherwise. We can turn this problem of expressing the E -tensors in terms of products of Kronecker deltas into a problem of combinatoric counting. We use the following tensors

$$\Delta_{ij}^2 = \delta_{ij} \quad (10)$$

$$\Delta_{ijkl}^4 = \delta_{ij}\delta_{kl} + \delta_{ik}\delta_{jl} + \delta_{il}\delta_{kj} \quad (11)$$

and so forth. Then we know that if E is isotropic it must be proportional to Δ

$$E^{(2n)} \propto \Delta^{(2n)} \quad (12)$$

and that the constant of proportionality may be obtained by counting the number of ways we could write a term comprising a product of n Kronecker deltas. Consider for example the case $n = 2$. Since the Kronecker delta is symmetric in

its indices, the following four products are identical: $\delta_{ij}\delta_{kl} = \delta_{ij}\delta_{lk} = \delta_{ji}\delta_{kl} = \delta_{ji}\delta_{lk}$. The degeneracy is 2^2 . Furthermore, the order of the Kronecker deltas also doesn't matter since they commute; that is, $\delta_{ij}\delta_{kl} = \delta_{kl}\delta_{ij}$. The degeneracy is $2!$. For the case where n is arbitrary, there are 2^n identical ways of writing the product of n Kronecker deltas. For each choice of indices, there are an additional $n!$ number of ways of ordering the products. Therefore, the total number of degeneracies equals $2^n n! = (2n)!!$. The total number of permutations for $2n$ indices equals $(2n)!$. So from this counting procedure we know that $\Delta^{(2n)}$ consists of a sum of $\frac{(2n!)}{(2n)!!} = (2n-1)!!$ terms.

The following relations will be very useful throughout later developments

$$E^1 = 0 \tag{13}$$

$$E^2 = \frac{B}{D} \delta_{ij} \tag{14}$$

$$E^3 = 0 \tag{15}$$

$$E^4 = \frac{B}{D(D+2)} (\delta_{ij}\delta_{kl} + \delta_{ik}\delta_{jl} + \delta_{il}\delta_{kj}) \tag{16}$$

In general, the lattice tensors are

$$E^{2n+1} = 0 \tag{17}$$

$$E^{2n} = \frac{B}{D(D+2) \cdots (D+2n-2)} \Delta^{2n} \tag{18}$$

5 Triangular Lattice

In a triangular lattice there are six vectors that we enumerate in this section by the following convention

$$\hat{\mathbf{e}}_{\mathbf{a}} = - \left(\sin \frac{\pi a}{3}, \cos \frac{\pi a}{3} \right), \tag{19}$$

where $a = 1, 2, \dots, 6$. The spatial coordinates of the lattice sites may be ex-

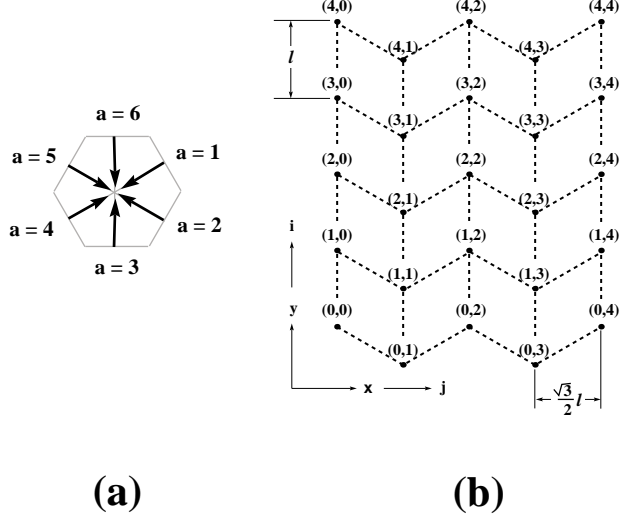


Figure 3: (a) Lattice vector label convention; (b) Hexagonal lattice convention with lattice directions $a = 3$ up and $a = 6$ down. Coordinates above the lattice nodes are (i, j) memory array indices.

pressed as follows

$$\mathbf{x}_{ij} = \left(\frac{\sqrt{3}}{2}j, i - \frac{1}{2}(j \bmod 2) \right) \quad (20)$$

where i and j are rectilinear indices which specify the data memory array location used to store the lattice-gas site data.

Let $s = (j \bmod 2)(r \bmod 2)$. Given a particle at site (i, j) , it may be shifted to a site r lattice units away to a remote site (i', j') by the following mapping

$$(i', j')_1 = \left(i + \frac{r+1}{2} - s, j - r \right) \quad (21)$$

$$(i', j')_2 = \left(i - \frac{r}{2} - s, j - r \right) \quad (22)$$

$$(i', j')_3 = (i - r, j) \quad (23)$$

$$(i', j')_4 = \left(i + \frac{r+1}{2} - s, j + r \right) \quad (24)$$

$$(i', j')_5 = \left(i - \frac{r}{2} - s, j + r \right) \quad (25)$$

$$(i', j')_6 = (i + r, j) \quad (26)$$

where $(i', j')_a$ denotes the shifted site, *i.e.* $(i, j) \rightarrow (i', j')$ with a shift along vector $\bar{\mathbf{r}} = r\hat{\mathbf{e}}_a$ and where division by 2 is considered integer division.

6 Local Collision Rules

In two-dimensions we may use a triangular lattice, with six bits per site encoding the occupation numbers of the six possible momentum states. Let n_a be the input bits and n'_a be the output bits of a local collision. A general collision operator is constructed as follows

$$\Omega_a = \sum_{\{\zeta_i\}} \alpha Q_a(\{\zeta_i\}), \quad (27)$$

where $\{\zeta_i\}$ is a set of occupied particle states and $\alpha = \pm 1$ is a scalar coefficient and where each term in the sum is written in factorized form as

$$Q_a(i_1, \dots, i_k) = \frac{n_{a+i_1}}{1-n_{a+i_1}} \dots \frac{n_{a+i_k}}{1-n_{a+i_k}} \prod_{j=1}^B (1-n_{a+j}). \quad (28)$$

Then the FHP collision operator is the following:

$$\Omega_a^{\text{FHP}} = \frac{1}{2}Q_a(1, 4) + \frac{1}{2}Q_a(2, 5) - Q_a(0, 3) + Q_a(1, 3, 5) - Q_a(0, 2, 4) \quad (29)$$

$$\begin{aligned} \Omega_0 &= \frac{1}{2}n_1n_4(1-n_0)(1-n_2)(1-n_3)(1-n_5) + \\ &\frac{1}{2}n_2n_5(1-n_0)(1-n_1)(1-n_3)(1-n_4) - \\ &n_0n_3(1-n_1)(1-n_2)(1-n_4)(1-n_5) + \\ &n_1n_3n_5(1-n_0)(1-n_2)(1-n_4) - \\ &n_0n_2n_4(1-n_1)(1-n_3)(1-n_5) \end{aligned}$$

Table 1: Simple right-handed collision table

n_0	n_1	n_2	n_3	n_4	n_5	n'_0	n'_1	n'_2	n'_3	n'_4	n'_5
1	0	0	1	0	0	0	0	1	0	0	1
0	1	0	0	1	0	1	0	0	1	0	0
0	0	1	0	0	1	0	1	0	0	1	0
1	0	1	0	1	0	0	1	0	1	0	1
0	1	0	1	0	1	1	0	1	0	1	0

Table 2: Simple left-handed collision table

n_0	n_1	n_2	n_3	n_4	n_5	n'_0	n'_1	n'_2	n'_3	n'_4	n'_5
1	0	0	1	0	0	0	1	0	0	1	0
0	1	0	0	1	0	0	0	1	0	0	1
0	0	1	0	0	1	1	0	0	1	0	0
1	0	1	0	1	0	0	1	0	1	0	1
0	1	0	1	0	1	1	0	1	0	1	0

Note that it is sufficient to give only Ω_0 since the other components of the collision operator can be obtained simply by incrementing the indices of Ω_0 owing to the six-fold symmetry of the collisions. The factors of one-half in (29) are transition probabilities for the 2-body collisions, indicating a coin toss is performed to choose between even or odd chirality.

The possible two-body and three-body collisions represented by (29) are illustrated in figure (4). For two-dimensional flow, there are four invariants, the mass, two components of the momentum, and the energy. With only the 2-body collision in figure (4), there is an additional invariant: the difference in the particle number along each of the three lattice directions. The 3-body collisions in figure (4) were include in the FHP-model to remove this spurious invariant. Consequently, the collisions enumerated in figure (4) are the minimally sufficient

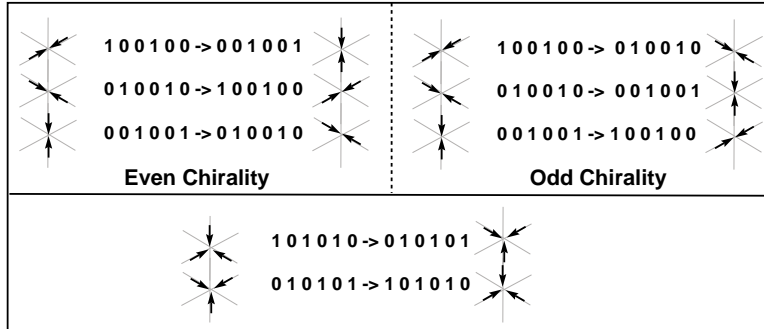


Figure 4: Enumeration of FHP 2-body collisions, even and odd chirality, and 3-body collisions.

set to produce hydrodynamic behavior in the continuum limit.

7 Long-Range 2-Body Interactions

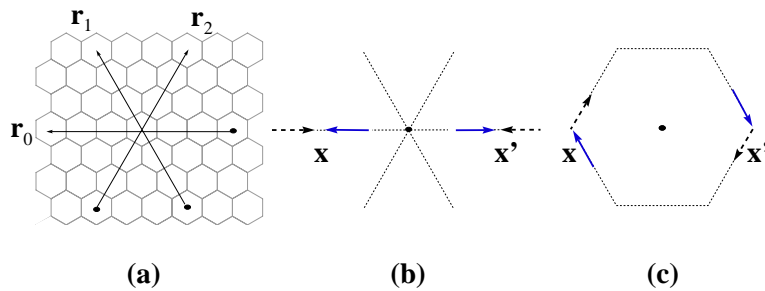


Figure 5: Simple bound-state orbits due to a long-range attractive interaction where the dotted path indicates the particle's closed trajectory: (a) partition directions; (b) bounce-back orbit with $|\Delta p| = 2$ and zero angular momentum; and (c) clockwise orbit with $|\Delta p| = 1$ and one unit of angular momentum. Head of the dashed arrows indicates particles entering the sites of partition \mathbf{r}_0 at time t . Tail of the black arrows indicates particles leaving those sites at time $t + \tau$. The counter-clockwise orbit is not shown.

An interparticle potential, $V(\mathbf{x} - \mathbf{x}')$, acts on particles spatially separated by a fixed distance, $\mathbf{x} - \mathbf{x}' = \mathbf{r}$. An effective interparticle force is caused by a non-local exchange of momentum. Momentum conservation is violated locally, yet it is exactly conserved in the global dynamics.

Table 3: Lattice vector components

a	x-component	y-component
0	-1	0
1	$-\frac{1}{2}$	$\frac{\sqrt{3}}{2}$
2	$\frac{1}{2}$	$\frac{\sqrt{3}}{2}$
3	1	0
4	$\frac{1}{2}$	$-\frac{\sqrt{3}}{2}$
5	$-\frac{1}{2}$	$-\frac{\sqrt{3}}{2}$

For the case of an attractive interaction, there exists a bound states in which two particles orbit one another. Since the particle dynamics are constrained by a crystallographic lattice we expect polygonal orbits. In figure 5 we have depicted two such orbits for a hexagonal lattice-gas. The range of the interaction is r . Two-body single range attractive interactions are depicted in figures 5b and 5c, the bounce-back and clockwise orbits respectively. Momentum exchanges occur along the principle directions. The interaction potential is not spherically symmetric, but has an angular anisotropy. In general, it acts only on a finite number of points on a shell of radius $\frac{r}{2}$. The number of lattice partitions necessary per site is half the lattice coordination number, since two particles lie on a line. Though microscopically the potential is anisotropic, in the continuum limit obtained after coarse-grain averaging, numerical simulation indicates isotropy is recovered.

8 A Simple Example: Bounce-Back Orbit

A long-range lattice-gas of the type we are considering still possesses the usual local dynamics of a hydrodynamic lattice-gas. To extend the local lattice-gas update rules to include long-range interactions, we use two additional bits of local site data. This will allow us to implement a long-range interaction using strictly local updating and therefore our algorithm will still be parallelizable just as a usual local lattice-gas. The two additional bits will denote the occupation numbers of messenger particles, or “photons”. The idea of using messenger particles was introduced by Appert *et al.*[8]. We have two types of messenger states, to represent incoming and outgoing conditions, and we denote the messengers as z_l and z_r .

Now for the simplest long-range lattice-gas model, we therefore use eight bits of local site data. Since long-range interactions occur between remote spatial sites, say \vec{x} and \vec{x}' , the messenger particles will travel either parallel or antiparallel to the vector $\vec{r} = \vec{x} - \vec{x}'$. All pairs of sites throughout the entire space that are separated by vector \vec{r} can therefore all be updated in parallel. We refer an update step of all pairs of 2-body interactions along direction \vec{r} as a *partition*, denoted by Γ_r . All possible two-body interaction pairs are then computed by performing all possible partitions of the space. So it requires many scans for the space to perform a single long-range interaction step.

In our two-dimensional example using a triangular lattice, there are three possible partitions. The number of partitions is never smaller than half the lat-

tice coordination number. In the two-dimensional case, the simplest long-range lattice-gas algorithm, though perhaps not the most efficient algorithm, is to use three *sequential* scans of the space, each scan performing the updating necessary for a single partition, see figure 5a. Often times, depending on the complexity of the long-range interactions and the dimensionality of the lattice, it is possible to perform *simultaneous* updating of multiple partitions. This of course is more desirable yet causes more complexity. Furthermore, this updating requires an extra pair of messenger particles for each partition to be simultaneously updated. For simplicity, we will not deal with this case here, however our implementation on the CAM-8 does use simultaneous partition updating—repulsive and attractive partitions are performed in parallel using four messenger bits.

Let us consider a simple example of the long-range lattice-gas algorithm, the minimal model of Appert. Here we consider only *bounce-back* attractive interactions. Suppose there is a single particle at site $\vec{x} = 0$ and there is also a single particle at site $\vec{x}' = r\hat{\mathbf{i}}$; that is, $n_0(\vec{x}) = 1$, $n_3(\vec{x}) = 0$, $n_0(\vec{x}') = 0$ and $n_3(\vec{x}') = 1$ with all other bits at \vec{x} and \vec{x}' being zero, see figure 5b. Here we are using the bit convention shown in table 3. Then the two particles are separated by a distance r and are moving away from each other. The attractive long-range interaction will effectively flip their respective directions making $n_0(\vec{x}) = 0$, $n_3(\vec{x}) = 1$, $n_0(\vec{x}') = 1$ and $n_3(\vec{x}') = 0$ so that the two particles will now be moving toward each other. There is a local momentum change of $2m\hat{\mathbf{c}}\mathbf{i}$ at \vec{x}' and an opposite momentum change of $-2m\hat{\mathbf{c}}\mathbf{i}$ at \vec{x} . Locally momentum is not conserved, but nonlocally it is.

The first step of the long-range interaction sequence is to choose a partition, say Γ_r , and then to emit messenger particles along the partition axis. The basic local rule for this first step is the following: a photon is emitted at a site if there exists a particle at that site that can partake in a long-range interaction. Another way of expressing this rule is: *send only if you can receive*. Obviously, for a particle to partake in an interaction there must be both a particle and a hole at that site. The factorized probability of having such a situation is just $d(1-d)$. So to continue with our example, for a photon to be emitted at some site \vec{x} parallel or antiparallel to a partition direction $\hat{\mathbf{i}}$, we use the following rule

$$z_r(\vec{x}) = n_0(\vec{x})(1 - n_3(\vec{x})) \quad (30)$$

$$z_l(\vec{x}) = n_3(\vec{x})(1 - n_0(\vec{x})). \quad (31)$$

Note that according to this local rule, only one photon can be created at a site, and consequently we eliminate the possibility of a long-range interaction, say of range $2r$, mediated through a doubly occupied site. The important consequence of the emission step, is that for two sites separated by the interaction distance, r , if both sites send photons, both will necessarily receive them, which strictly enforces nonlocal momentum conservation. *Give and ye shall receive* (provided your's is received). Letting $z_a \equiv z_r$ and $z_{-a} \equiv z_l$, in general we can write the emission step of the minimal interaction as

$$z_a(\vec{x}) = n_{-a}(\vec{x})(1 - n_a(\vec{x})), \quad (32)$$

where $a = 0, 1, 2$ covers all the partitions.

After the emission step, follows a long-range kick of the messenger bits. In

the simple example, all photons z_l are kicked along $-r\hat{\mathbf{i}}$ and all photons z_r are kicked along $r\hat{\mathbf{i}}$. In general for the long-range kick we have

$$z'_a(\vec{x} + r\hat{e}_a) = z_a(\vec{x}). \quad (33)$$

Finally, we have the absorption step of the long-range interaction sequence. Here the local particle momentum state is updated as the particles flip their directions in our example

$$n'_3(\vec{x}) = n_3(\vec{x}) + z'_l(\vec{x})n_0(\vec{x})(1 - n_3(\vec{x})) - z'_r(\vec{x})n_3(\vec{x})(1 - n_0(\vec{x})) \quad (34)$$

$$n'_0(\vec{x}) = n_0(\vec{x}) + z'_r(\vec{x})n_3(\vec{x})(1 - n_0(\vec{x})) - z'_l(\vec{x})n_0(\vec{x})(1 - n_3(\vec{x})). \quad (35)$$

Moreover, in this step all the messenger bits are set to zero throughout the entire space. For any direction, the local absorption rule could more simply be written as

$$n'_a(\vec{x}) = n_a(\vec{x}) + z'_{-a}(\vec{x})z_a(\vec{x}) - z'_a(\vec{x})z_{-a}(\vec{x}). \quad (36)$$

Substituting in (32) and (33) into (36), we have a single boolean expression in terms of number variables for a single long-range interaction step for partition Γ_r as follows

$$\begin{aligned} n'_a(\vec{x}) = & n_a(\vec{x}) + \\ & n_a(\vec{x} + r\hat{e}_a)(1 - n_{-a}(\vec{x} + r\hat{e}_a))n_{-a}(\vec{x})(1 - n_a(\vec{x})) - \\ & n_{-a}(\vec{x} - r\hat{e}_a)(1 - n_a(\vec{x} - r\hat{e}_a))n_a(\vec{x})(1 - n_{-a}(\vec{x})) \end{aligned} \quad (37)$$

Table 4: Long-range interaction sequence

events	$n_a(x)$	$z_l(x)$	$z_r(x)$	$n_a(x')$	$z_l(x')$	$z_r(x')$
initial	100000	0	0	000100	0	0
emit	100000	0	1	000100	1	0
kick	100000	1	0	000100	0	1
absorb	000100	0	0	100000	0	0

For convenience we define a long-range collision operator, P_a , as follows

$$P_a(\vec{x}) = z'_{-a}(\vec{x})z_a(\vec{x}), \quad (38)$$

so that we may write

$$n'_a(\vec{x}) = n_a(\vec{x}) + P_a(\vec{x}) - P_{-a}(\vec{x}). \quad (39)$$

The state data for this simple example we have been considering is given in table 4, which represents all the steps of a long-range interaction sequence for a partition along the x-axis.

9 Another Example: Clockwise Orbit

To continue illustrating our implementation of a long-range lattice-gas, in this section we again consider a system with a single attractive interaction of range r , however the local momentum states participating in the interaction are not along the partition direction. Yet in the example given here, the momentum exchange is still along the partition direction so that the long-range interaction remains a central-body one, resulting in a bound state with two particles trapped in a clockwise orbit. (Note that the restriction to central-body forces is not necessary, but is presented here for convenience.) In this slightly more

complicated example, the local rules for photon emission, and absorption, (32) and (36) respectively, have a more general form with the implication that the emission and absorption of photons is different from the previous example of the bounce-back orbit and should be noted when making look-up tables to do this computation. The local photon emission rules can be written

$$z_a(\vec{x}) = n_c(\vec{x})(1 - n_d(\vec{x})) \quad (40)$$

$$z_{-a}(\vec{x}) = n_g(\vec{x})(1 - n_h(\vec{x})) \quad (41)$$

where the bits c, d, g, h must be chosen so momentum is conserved

$$\hat{e}_c - \hat{e}_d + \hat{e}_g - \hat{e}_h = 0 \quad (42)$$

as well as be constrained by central-body parallel and perpendicular momentum exchange conditions

$$(\hat{e}_c - \hat{e}_d - \hat{e}_g + \hat{e}_h) \cdot \vec{r} = 2\Delta p \quad (43)$$

$$(\hat{e}_c - \hat{e}_d - \hat{e}_g + \hat{e}_h) \times \vec{r} = 0, \quad (44)$$

where Δp is the momentum change per site due to the long-range interaction. In (40) and (41) the difference, over our previous example of the bounce-back orbit, is the possibility of having two-photons emitted at a single site.

To be explicit, for the two-dimensional triangular lattice, we can satisfy (42), (43), and (44) by choosing the indices c, d, g, h as follows:

$$c = a - 2 \quad (45)$$

$$d = a - 1 \quad (46)$$

$$g = -c \quad (47)$$

$$h = -d. \quad (48)$$

An example of this choice of indices is illustrated in figure 5c. Then the emission rule, (40) and (41), is simply

$$z_a(\vec{x}) = n_{a-2}(\vec{x})(1 - n_{a-1}(\vec{x})) \quad (49)$$

Since the kicking of the photons is the same in this example as in the previous one, (33) still holds

$$z'_a(\vec{x} + r\hat{e}_a) = z_a(\vec{x}).$$

By re-expressing (36) more generally, we can write a local absorption rule

$$n'_a(\vec{x}) = n_a(\vec{x}) + z'_{-(a+1)}(\vec{x})z_{a+1}(\vec{x}) - z'_{a-1}(\vec{x})z_{-(a-1)}(\vec{x}) \quad (50)$$

or more elegantly

$$n'_a(\vec{x}) = n_a(\vec{x}) + P_{a+1}(\vec{x}) - P_{-a+1}(\vec{x}). \quad (51)$$

Substituting in (49) and (33) into (50) and after some manipulation of the indices, we have a single boolean expression in terms of number variables for a single long-range interaction step for partition Γ_r as follows

$$\begin{aligned} n'_a(\vec{x}) &= n_a(\vec{x}) + \\ & n_{a+2}(\vec{x} + r\hat{e}_{a+1})(1 - n_{-a}(\vec{x} + r\hat{e}_{a+1}))n_{a-1}(\vec{x})(1 - n_a(\vec{x})) - \\ & n_{-a}(\vec{x} - r\hat{e}_{a-1})(1 - n_{a-2}(\vec{x} - r\hat{e}_{a-1}))n_a(\vec{x})(1 - n_{a+1}(\vec{x})). \end{aligned}$$

Table 5 gives the local site data for the x-axis partition of a clock-wise orbit. The particle $n_4(\vec{x})$ acts as a kind of spectator in this example, illustrating that

Table 5: Long-range interaction sequence with two photons emitted at a single site

labels	$n_a(x)$	$z_l(x)$	$z_r(x)$	$n_a(x')$	$z_l(x')$	$z_r(x')$
events	010010	0	0	000010	0	0
emit	010010	1	1	000010	1	0
kick	010010	1	0	000010	0	1
absorb	001010	0	0	000001	0	0

Table 6: Long-range interaction sequence with two photons emitted and absorbed at site \mathbf{x}' in a back-to-back interaction

events	$n_a(x)$	$z_l(x)$	$z_r(x)$	$n_a(x')$	$z_l(x')$	$z_r(x')$	$n_a(x'')$	$z_l(x'')$	$z_r(x'')$
initial	010000	0	0	010010	0	0	000010	0	0
emit	010000	0	1	010010	1	1	000010	1	0
kick	010000	1	0	010010	1	1	000010	0	1
absorb	001000	0	0	001001	0	0	000001	0	0

two photons can be emitted from a single site. It is also possible to have two photons absorbed at a single site. Let us consider a *back-to-back* interaction over three sites. Suppose there are particles at sites $\vec{x} = 0$, $\vec{x}' = r\hat{\mathbf{i}}$, and $\vec{x}'' = 2r\hat{\mathbf{i}}$. Table 6 gives the site data for these sites were there are two photons emitted and absorbed at \vec{x}' in the middle location.

The minimal model using only a attractive interactions models a fluid with liquid and gas phases at zero temperature. Figure 6 shows the time evolution of the phase separation process in this case at a density $d = 0.07$ and interaction range $r = 6l$ and illustrates the type of physical simulation that can be achieved with the simplest long-range lattice-gas algorithm.

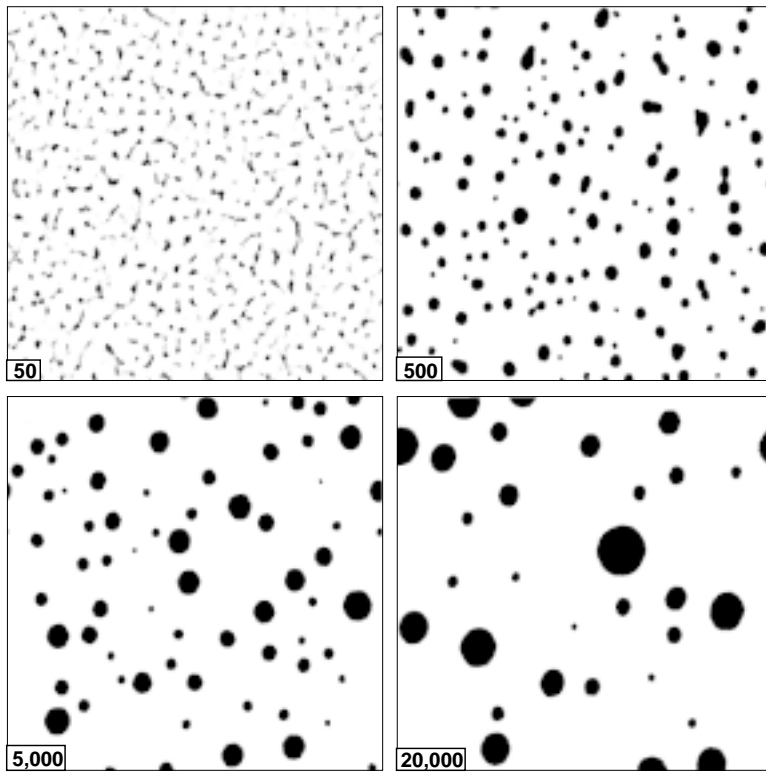


Figure 6: Time evolution of a liquid-gas phase separation for a lattice-gas with long range attractive interactions at range $r = 6$ on a 1024×1024 lattice starting with a uniformly random configuration of density $d = 0.07$.

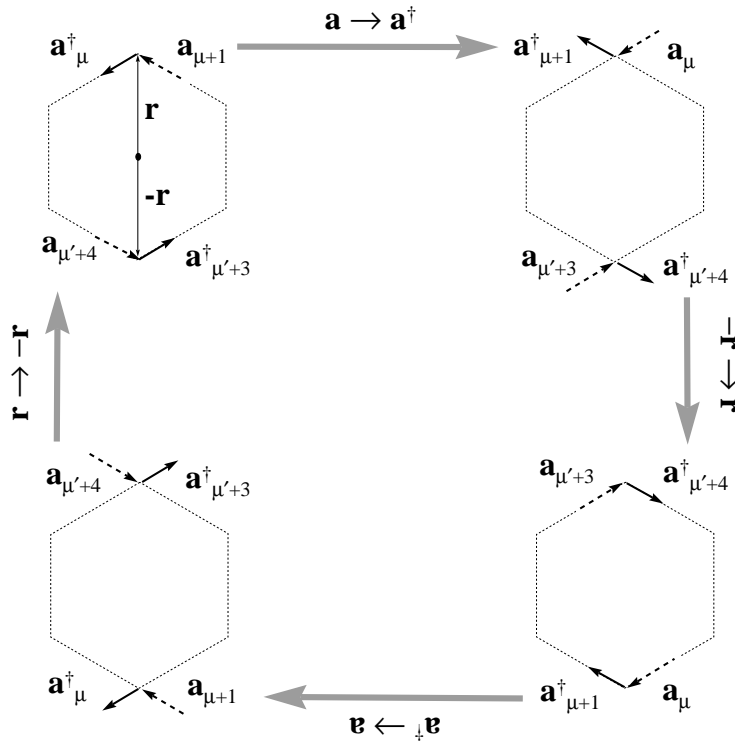


Figure 7: Examples of two-body finite impact parameter collisions along the \mathbf{r}_0 -direction. The four terms of interaction Hamiltonian for $|\Delta p| = 1$. Dashed arrows depict input states and black arrows depict output states.

10 Symmetries in Long Range Interactions

For the case of an attractive interaction as mentioned earlier, we would expect that there exists a bound state in which two particles orbit one another, for example the clockwise orbit shown in figure 5c. The range of the interaction is r . This hexagonal orbit is also shown in the bottom-right corner of figure 7. In this figure the hexagon's radius is also labeled as r and should not be confused with the interaction range which is the hexagon's diameter. Similarly a counter-clockwise orbit is possible, see the top-left corner of figure 7. A time-reversal invariance exists between these two cases with respect to conjugation and parity operations as depicted in figure 7.

These diagrams describe the possible 2-body collisions that can be so generated, including repulsive interactions. This logical correspondence between the different type of 2-body interactions, allows one to achieve a more efficient implementation of a long-range lattice-gas algorithm than what we have achieved on the CAM-8 since we have not used this form of logical economy. Furthermore, there is a correspondance property for $r = 0$, the situation reduces to the 2-body collisions in the FHP lattice-gas ².

The long range interactions considered here have the following properties which simplify a computational implementation: 1) there exists only parallel momentum exchange, a restriction for modelling central body forces; 2) the interaction acts only along the principal lattice directions; 3) there exists time-

²For $r = 0$, the $|\Delta p| = 1$ interactions reduce to a rotation of the states, $\mathcal{R}(\frac{\pi}{3})$ and $\mathcal{R}(\frac{2\pi}{3})$; and the $|\Delta p| = 2$ interactions reduce to the identity operation.

reversal invariance with respect a conjugation and parity operations; and 4) a bias to the interactions can be assigned by coupling to heat-bath states. In our previous examples, the bounce-back and clockwise orbits, we discussed properties 1 and 2. In this section we have discussed property 3. We have discussed property 4 elsewhere [9].

11 Central-Body Interaction Neighborhood and 2D Crystallization

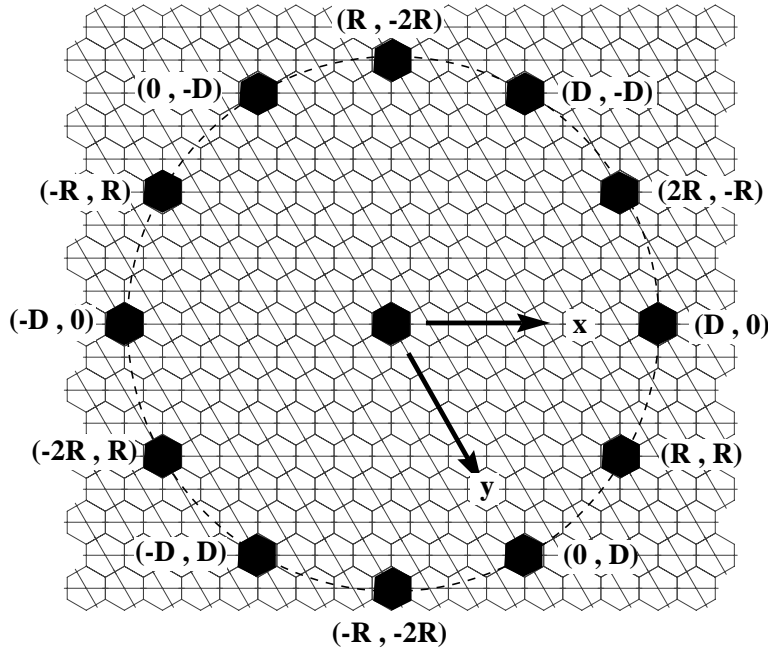


Figure 8: Twelve neighbors on a triangular lattice that can participate in long-range central-body interactions. Interaction range $D = 7$ is depicted, where $R = \frac{D}{\sqrt{3}} \simeq 4$ to within 1.03 percent error. Computer memory space coordinates (x, y) are given adjacent to each neighboring site.

In the previous two sections we illustrated two examples of the long-range in-

interactions, the bounce-back and clockwise orbit on a two-dimensional triangular lattice. In general, the long-range interaction step will involve many partitions, both attractive and repulsive interactions, and multiple ranges. In our CAM-8 implementation of a long-range lattice-gas with central-body interactions, we actually use 12 neighbors in two-dimensions, see figure 8. The triangular lattice is superposed over a square lattice, which appears rhomboidal in the figure. The square lattice is often used for embedding the site data into computer memory, which is rectilinear. This kind of embedding is the simplest and used for simulations that possess periodic boundary conditions. The reason for using 12 neighbors is to try to achieve a higher degree of local symmetry. In doing molecular dynamics modeling with a multi-long-range lattice-gas, we have found that 12 neighbors are necessary to recover macroscopic isotropy. In particular, 12 neighbors are necessary to have the emergent crystalline solid be able to freely rotate in space. A mean-field analysis of the lattice-gas crystallization method has been presented elsewhere [10]. Figure 8 shows a *ring* of range 7 lattice spacings.

To implement the crystallization algorithm, we use up to eight ranges in two-dimensions. That is, eight rings of the type shown in figure 8 for a total of 96 neighbors. Half the rings are used for attractive interactions and the other half are used for repulsive interactions. Typically, the inner rings are attractive, the middle rings are repulsive, and the outer rings are again attractive. Since four photon bits are used in our implementation, and since each ring is either attractive or repulsive, two rings are affected by a simultaneous parti-

tioning of the space. For the attractive interaction, there are 5 type of orbits: bounce-back with $\Delta p = 2$, clockwise and counter-clockwise with $\Delta p = 1$, and clockwise and counter-clockwise with $\Delta p = \sqrt{3}$. Consequently, there are 5 types of repulsive interactions, which are just the conjugates of the 5 attractive ones. Since there are 3 partition directions for a triangular lattice, it takes $5*3=15$ partitions of the space to completely update an attractive ring and a repulsive ring simultaneously. To compute 8 rings therefore takes $4*15=60$ scans of the space. Therefore, since the local collisions require a single scan, it takes a total of 61 scans to complete one time step.

A two dimensional example using 6 interaction ranges, with an underlying 512×512 lattice, of this time-dependent crystallization process is given in figure 9 and illustrates the type of molecular dynamics simulation that can be achieved with a more complex long-range lattice-gas algorithm. The resulting crystal is in a hexagonal-close-pack configuration since we have strived to make the coarse-grained interatomic potential be radially symmetric. This long-range lattice-gas model had six interaction ranges: $r = -2, -7, 19, 21, -24, -26$. Here the negative sign preceding the range denotes an attractive interaction at that range.

12 Conclusion

Although the lattice-gas molecular dynamics algorithm, described above, requires 61 scan, which is quite a lot of scans, this implementation only requires 10 bits of local site data. Six bits are used for the momentum states and 4 bits

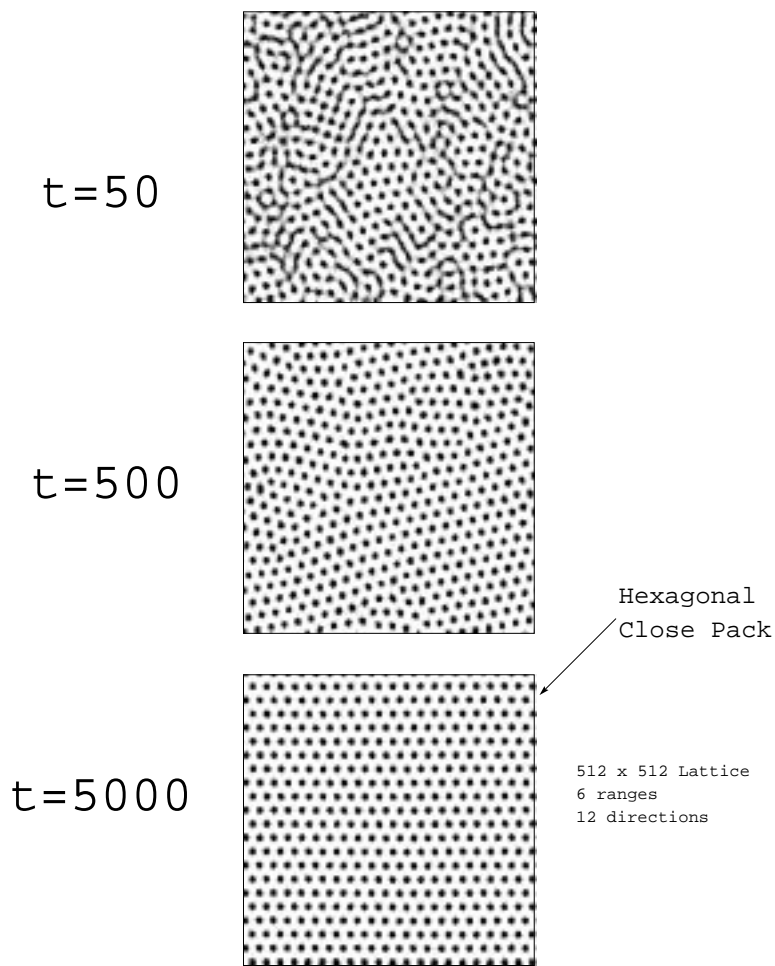


Figure 9: Time evolution of crystallization in a 2-dimensional lattice-gas with multiple fixed-range 2-body interactions. The resulting crystal is in a hexagonal-close-pack configuration since the coarse-grained interatomic potential is radially symmetric. The underlying lattice is 512×512 . Started with a uniformly random configuration at $d = 0.1$. Twelve directions are used for long-range momentum exchanges. Grain boundaries and defects are observed during the early stages of the crystal formation.

for messenger states, which means that only 1K byte is needed to store a long-range rule. Since the CAM-8 uses a 16-bit word, there still remains 6 bits of unused local data. We use these remaining bits to hold a table look-up *address*. That is, since the size of the CAM-8 look-up table static random access memory (SRAM) is 64K bytes, and our long-range rule only requires 1K bytes, we can store up to 64 long-range rules into CAM-8's SRAM memory. Since our molecular dynamics algorithm decomposes into 61 applications of the long-range rules, it is now clear why we have chosen to use up to eight ranges. Although the description of our implementation may sound complicated, in fact from a software development point-of-view it was the most direct and most simple. We have traded off time to save memory. Yet the well-known principle of computer science that one can save much time at the expense of using more memory applies to our algorithm. So optimizations of our algorithm can be made, particularly concerning trading off an increase of local site data for a decrease in the number of needed scans. Clearly, the molecular dynamics algorithms would be significantly sped-up if it were implemented say on a 64-bit architecture. Of course in this case, computation by table look-up would be inappropriate. However by making use of lattice isometries and rule conjugation, the necessary logic is actually quite small, as evidenced for example by (37) or (52). Therefore, a programmable logic method of computation should be better than the table look-up method of computation currently in use in the CAM-8 for this kind of lattice-gas algorithm.

References

- [1] Uriel Frisch, Brosl Hasslacher, and Yves Pomeau. Lattice-gas automata for the navier-stokes equation. *Physical Review Letters*, 56(14):1505–1508, 1986.
- [2] Norman Margolus and Tommaso Toffoli. Cellular automata machines. In Gary D. Doolean, editor, *Lattice Gas Methods for Partial Differential Equations*, pages 219–249. Santa Fe Institute, Addison-Wesley Publishing Company, 1990. The first 8-module CAM-8 prototype was operational in the fall of 1992.
- [3] Norman Margolus. Cam-8: a computer architecture based on cellular automata. *American Mathematical Society*, 6, 1996. Fields Institute Communications.
- [4] Tommaso Toffoli. Cam: A high-performance cellular-automaton machine. *Physica*, 10D:195–204, 1984. A demonstration TM-gas experiment was part of the CAMForth software distribution.
- [5] Tommaso Toffoli and Norman Margolus. *Cellular Automata Machines*. MIT Press Series in Scientific Computation. The MIT Press, 1987.
- [6] Norman Margolus, Tommaso Toffoli, and Gérard Vichniac. Cellular-automata supercomputers for fluid-dynamics modeling. *Physical Review Letters*, 56(16):1694–1696, 1986.

- [7] Stephen Wolfram. Cellular automaton fluids 1: Basic theory. *Journal of Statistical Physics*, 45(3/4):471–526, 1986.
- [8] Cécile Appert, Dominique d’Humières, Valérie Pot, and Stéphane Zaleski. Three-dimensional lattice gas with minimal interactions. In *Transport Theory and Statistical Physics*, volume 23 (1-3), pages 107–122. Proceedings of Euromech 287 - Discrete Models in Fluid Dynamics, New York, M. Dekker, 1994. Editor P. Nelson.
- [9] Jeffrey Yepetz. A lattice-gas with long-range interactions coupled to a heat bath. *American Mathematical Society*, 6:261–274, 1996. Fields Institute Communications.
- [10] Jeffrey Yepetz. Lattice-gas crystallization. *Journal of Statistical Physics*, 81(1/2):255–294, 1994.